Photochemistry and Photobiology, 1997, 65(1): 96–102

Photooxidation of Tryptophan: $O_2(^1\Delta_g)$ *versus* Electron-Transfer Pathway

Jurina M. Wessels*[1], Christopher S. Foote[1], William E. Ford[2] and Michael A. J. Rodgers[2]

[1]Department of Chemistry and Biochemistry, University of California, Los Angeles, Los Angeles, CA, USA and
[2]Center for Photochemical Sciences, Bowling Green State University, Bowling Green, OH, USA

Received 30 July 1996; accepted 9 October 1996

ABSTRACT

Tris (2,2′-bipyridyl)ruthenium(II)chloride hexahydrate ($Ru[bpy]_3^{2+}$) free in solution and adsorbed onto antimony-doped SnO_2 colloidal particles was used as a photosensitizer for a comparison of the $O_2(^1\Delta_g)$ and electron-transfer-mediated photooxidation of tryptophan (TRP), respectively. Quenching of excited $Ru(bpy)_3^{2+}$ by $O_2(^3\Sigma_g^-)$ in an aerated aqueous solution leads only to the formation of $O_2(^1\Delta_g)$ (ϕ_Δ = 0.18) and this compound was used as a type II photosensitizer. Excitation of $Ru(bpy)_3^{2+}$ adsorbed onto Sb/SnO_2 results in a fast injection of an electron into the conduction band of the semiconductor and accordingly to the formation of $Ru(bpy)_3^{2+}$ and was used for the sensitization of the electron-transfer-mediated photooxidation. The $Ru(bpy)_3^{3+}$ is reduced by TRP with a bimolecular rate constant $k_Q = 5.9 \times 10^8\ M^{-1}\ s^{-1}$, while $O_2(^1\Delta_g)$ is quenched by TRP with $k_t = 7.1 \times 10^7\ M^{-1}\ s^{-1}$ (chemical + physical quenching). Relative rate constants for the photooxidation of TRP (k_c) *via* both pathways were determined using fluorescence emission spectroscopy. With N_p, the rate of photons absorbed, being constant for both pathways we obtained $k_c = (372/N_p)\ M^{-1}\ s^{-1}$ for the $O_2(^1\Delta_g)$ pathway and $k_c \geq (25\,013/N_p)\ M^{-1}\ s^{-1}$ for the electron-transfer pathway, respectively. Thus the photooxidation of Trp is more than two orders of magnitude more efficient when it is initiated by electron transfer than when initiated by $O_2(^1\Delta_g)$.

INTRODUCTION

Energy transfer from an excited triplet state of a photosensitizer to molecular oxygen $O_2(^3\Sigma_g^-)$ and the subsequent production of the metastable excited state, $O_2(^1\Delta_g)$, as well as electron transfer between an excited triplet state of a photosensitizer and a substrate molecule can initiate photooxidation reactions of biomolecules. These two mechanisms are commonly referred to as the type II and type I mechanism, respectively (1).

Proteins are one of the cellular constituents that are susceptible to photooxidation reactions. The photooxidation of amino acid side chains can cause significant alterations in the physicochemical properties of proteins and can subsequently lead to cellular damage (2–5). It has been shown that, besides tryptophan (TRP)†, histidine, cysteine, methionine and tyrosine are vulnerable to photodynamic action (6). The products of the photooxidation reactions as well as the reaction pathway are strongly dependent on the photophysical properties of the sensitizer as well as on the properties of the substrate molecule (7,8). Furthermore the reaction pathway is dependent on the solvent, the pH and the temperature (8–12). The $O_2(^1\Delta_g)$ photooxidation reaction of TRP has been studied extensively (13–17). It has been demonstrated that rate constants for the chemical as well as physical quenching of $O_2(^1\Delta_g)$ by TRP depend not only on the accessibility of the reaction site, *i.e.* whether it is buried in the interior of the protein (18) or tied up in peptide bonds (19–21), but also strongly on the medium polarity (9,10,12,22).

Besides the $O_2(^1\Delta_g)$ pathway the type I mechanism has been suggested to be responsible for the photooxidation of TRP *via* certain sensitizers (7,11,12,23,24). Thermodynamic arguments have been advanced that indicate that the primary targets of type I processes are those amino acids that are most readily oxidized in electron transfer situations (tyrosine, TRP, methionine, cysteine) (25).

The efficiency of photooxidations *via* the $O_2(^1\Delta_g)$ pathway or the radical pathway and the problem of distinguishing between type I and type II has been discussed by Foote (1). In view of the fact that the product distribution as well as the favored pathway depends on the reduction potentials of the sensitizer and substrate molecule, we were interested in a comparison of the rate constant for the $O_2(^1\Delta_g)$-mediated photooxidation of TRP with that of a radical-mediated pathway for the photooxidation of TRP using the same sensitizer for both pathways.

It has been shown that tris (2,2′-bipyridyl)ruthenium-(II)chloride hexahydrate ($Ru[bpy]_3^{2+}$) is an efficient photosensitizer (26). Two mechanisms have been reported for the quenching of the excited-state $*Ru(bpy)_3^{2+}$ by ground-state oxygen:

$$*Ru(bpy)_3^{2+} + O_2(^3\Sigma_g^-) \rightarrow Ru(bpy)_3^{3+} + O_2^{\cdot-} \quad (1)$$

$$*Ru(bpy)_3^{2+} + O_2(^3\Sigma_g^-) \rightarrow Ru\ (bpy)_3^{2+} + O_2(^1\Delta_g) \quad (2)$$

*To whom correspondence should be addressed at: GSF-Research Center for Health and Environment, Ingolstädter Landstr. 1, 85764 Oberschleißheim, Germany. Fax: 49-89-3187/3426; e-mail: wessles@gsf.de.

†*Abbreviations:* HPI, hydroperoxy-hydropyrrole-indole carboxylic acid; N-FK, *N*-formylkynurenin N_P, rate of photon absorption; $Ru(bpy)3^{2+}$, tris(2,2′-bipyridyl)ruthenium(II)chloride hexahydrate; TRP, tryptophan.

The yield of the first process is negligible as a result of an efficient back electron transfer within the solvent cage (27). The quantum efficiency for the generation of $O_2(^1\Delta_g)$ in H_2O is 0.5 (26).

When the $Ru(bpy)_3^{2+}$ complex is adsorbed onto an antimony-doped SnO_2 semiconductor particle, the excited-state lifetime is shortened due to injection of an electron into the conduction band of the semiconductor. This process reduces the lifetime of the excited state of the complex to *ca* 1 ns (28).

$$Ru(bpy)_3^{2+} + h\nu \rightarrow {}^*Ru(bpy)_3^{2+} \rightarrow Ru(bpy)_3^{3+} + e^-(SnO_2) \quad (3)$$

Thus the injection of an electron results in the rapid formation of the oxidized $Ru(bpy)_3^{2+}$ complex, $Ru(bpy)_3^{3+}$. The reduction potential of the $Ru(bpy)_3^{3+}/Ru(bpy)_3^{2+}$ couple is + 1.26 V *vs* NHE (29). The $Ru(bpy)_3^{3+}$ can oxidize electron donors such as TRP that has a redox potential of E^0 = 1.015 V *vs* NHE at pH 7 (30). This reaction competes with the recapture of the conduction band electron by the $Ru(bpy)_3^{3+}$, which is on the order of 4×10^5 s^{-1}. In this study we present kinetic studies on the photooxidation of TRP *via* $O_2(^1\Delta_g)$ as well as *via* an electron-transfer pathway using $Ru(bpy)_3^{2+}$ free in solution or adsorbed onto a semiconductor surface as a photosensitizer (Eqs. 2 and 3).

MATERIALS AND METHODS

Materials. L-tryptophan and $Ru(bpy)_3^{2+}$ were obtained from Aldrich and used as received. Antimony-doped SnO_2 colloidal suspension (15% in H_2O) was used as received from Alfa and characterized as described previously (31). The final concentration of antimony-doped SnO_2 particles, calculated based on a particle size of 4 nm and a density of 6.95 g cm^{-3} (31) in a 23 μM solution of $Ru(bpy)_3^{2+}$ was approximately 12.5 μM. Under these conditions, essentially all (99 ± 1%) of the $Ru(bpy)_3^{2+}$ is adsorbed onto the surface of the SnO_2 particles (30).

Laser-flash photolysis experiments. The excited-state lifetime of $Ru(bpy)_3^{2+}$ in the absence and presence of 13.8 mM TRP was measured by monitoring the decay of the excited state of $Ru(bpy)_3^{2+}$ in solution by monitoring its emission at 610 nm. The $Ru(bpy)_3^{2+}$ was excited using a frequency-doubled Q-switched Nd:YAG laser (Continuum Surelite) (532 nm, *ca* 7 ns pulse width). The absorbance of the sample at the excitation wavelength was ~0.03 (per cm). The lifetime of $Ru(bpy)_3^{3+}$ in the absence and presence of various TRP concentrations was monitored at 450 nm as recovery of the ground state after the initial bleaching.

Kinetic measurements. One milliliter samples of 23 μM solutions of $Ru(bpy)_3^{2+}$ or $Ru(bpy)_3^{2+}/SnO_2$ and 59.3 μM TRP were illuminated simultaneously in quartz cuvettes using the 514 nm line of an Ar^+ laser (355 mW/cm^2). During illumination, samples were continuously bubbled with compressed air. The laser light was brought to the samples *via* a fiber optic. The polished fiber end was imaged *via* a planoconvex lens onto the illumination area of approximately 8 cm^2. After a chosen illumination time 100 µL of the sample were diluted with 1.1 mL double-distilled H_2O. Fluorescence emission measurements were performed using a SPEX Fluorolog spectrophotometer. The excitation and emission slits were set to 2 mm and 3 mm, respectively. The TRP fluorescence was excited at 290 nm and the fluorescence intensity was evaluated at 368 nm. Calibration curves were measured for both sensitizer systems, *i.e.* $Ru(bpy)_3^{2+}$ free in solution and adsorbed onto SnO_2 particles. The emission intensity in the samples containing SnO_2 particles was slightly reduced compared to the samples without the particles. This decrease in the fluorescence intensity was independent of the TRP concentration, indicating that this is not a result of an interaction between TRP and the SnO_2 particles. The decrease in the fluorescence intensity can be attributed to the strong competing absorbance of the SnO_2 particles at 290 nm (valence conduction band transition). The SnO_2 particles have a diameter of 4 nm and the light scattering at the excitation wavelength is negligible (31). The uncertainty in the determination of the TRP concentration *via* fluorescence emission measurements was determined to be 6% from a set of eight experiments. The absorbance of the $Ru(bpy)_3^{2+}$ solution at 514 nm was ~0.03 (per cm). Kinetic studies of the photooxidation of TRP *via* both pathways were performed in double-distilled H_2O using a TRP concentration of 59.3 μM. All solutions were prepared and kept in the dark before the measurements. All measurements were carried out at room temperature (20 ± 1°C) and the samples were bubbled with compressed air during the measurements.

NMR spectroscopic measurements. For a qualitative comparison of the photooxidation products, ^{1}H-NMR measurements were performed using an AM 500 nuclear magnetic resonance spectrometer (Bruker). For ^{1}H-NMR measurements, solutions of $Ru(bpy)_3^{2+}$ and $Ru(bpy)_3^{2+}/SnO_2$ were prepared in D_2O and illuminated at 514 nm as described above for 3 h with 355 mW/cm^2. The samples were continuously bubbled with compressed oxygen during illumination.

RESULTS AND DISCUSSION

Sensitization of $O_2(^1\Delta_g)$ by $Ru(bpy)_3^{2+}$

As described above, the metal-to-ligand charge transfer excited state of $Ru(bpy)_3^{2+}$ can be quenched by $O_2(^3\Sigma_g^-)$ *via* electron transfer (Eq. 1) and energy transfer (Eq. 2). As a result of rapid electron back transfer between the redox products, only $O_2(^1\Delta_g)$ can be detected as a product of the quenching reaction in aqueous solutions (26,27). In order to validate that the excited state of $Ru(bpy)_3^{2+}$ is not quenched by TRP, measurements of the excited-state lifetime were performed in the presence and in the absence of TRP.

The $Ru(bpy)_3^{2+}$ complex in aqueous solution was excited at 532 nm (~7 ns). The decay of the excited state with and without TRP was detected at 610 nm. In aerated H_2O solution a monoexponential decay to the baseline was observed in the presence (τ = 383 ± 24 ns) of 11.5 mM TRP and in its absence (τ = 365 ± 6 ns), indicating that the excited state of $Ru(bpy)_3^{2+}$ is not quenched by the presence of the TRP concentrations used, and thus only $O_2(^1\Delta_g)$ can be generated in aqueous solution.

As a result of the competition between electron- and energy transfer the quantum efficiency of $O_2(^1\Delta_g)$ generation from $Ru(bpy)_3^{2+}$ in H_2O is 0.5 (26). The yield of singlet oxygen production in air-saturated water can be calculated taking into account the probability of the quenching of $^*Ru(bpy)_3^{2+}$ by O_2 in competition with the intrinsic decay process according to

$$\phi_\Delta = 0.5 \frac{k_{ET}[O_2]}{k_0 + k_{ET}[O_2]} \quad (4)$$

where k_{ET} is the bimolecular rate constant for energy transfer from $^*Ru(bpy)_3^{2+}$ to O_2, k_0 is the inverse of the intrinsic lifetime of $^*Ru(bpy)_3^{2+}$ and $[O_2]$ is the concentration of molecular oxygen in H_2O. In aerated water with the values of the parameters being $[O_2] = 2.7 \times 10^{-4}$ M, $k_{ET} = 3.4 \times 10^9$ $M^{-1}s^{-1}$ and $k_0 = 1.64 \times 10^6$ s^{-1} (26), the quantum yield of singlet oxygen formation is ϕ_Δ = 0.18, which represents *ca* 35% of the maximum value of 0.5.

The total rate constant for quenching of $O_2(^1\Delta_g)$ by TRP (k_t) is the sum of the physical, nonreactive quenching k_P (Eq. 5) and the chemical quenching k_c (Eq. 6):

$$O_2(^1\Delta_g) + TRP \rightarrow O_2(^3\Sigma_g^-) + TRP,\ k_P \quad (5)$$

$$O_2(^1\Delta_g) + TRP \rightarrow TRP{\cdot}O_2,\ k_c \quad (6)$$

Table 1. Rate constants for the $Ru(bpy)_3^{2+}$ and $Ru(bpy)_3^{2+}/SnO_2$-sensitized photooxidation of TRP and quantum yields for $O_2(^1\Delta_g)$ and TRP^{+} at [TRP] = 59 μM*

$Ru(bpy)_3^{2+}$	k_{ET} (M^{-1} s^{-1})	k_0 (s^{-1})	ϕ_Δ	k_t (M^{-1} s^{-1})	k_Δ^0 (s^{-1})
	3.4×10^9	1.64×10^6	0.18	7.1×10^7	2.5×10^5
$Ru(bpy)_3^{2+}/$ SnO_2	k_Q (M^{-1} s^{-1})	k_{REC} (s^{-1})	$\phi_{TRP^{+}}$		
	5.9×10^8	4.0×10^5	0.075		

*k_{ET} and k_0 were obtained from Mulazzani et al. (26).

From time-resolved measurements of the $O_2(^1\Delta_g)$ lifetime in nonbuffered D_2O in the absence and presence of various TRP concentrations up to 1.2 mM, we obtained a rate constant for the quenching of $O_2(^1\Delta_g)$ by TRP of $k_t = 7.1 \times 10^7$ M^{-1} S^{-1} (data not shown), which is within the range of values published in the literature (10,11,32,33). The rate constants of the $O_2(^1\Delta_g)$ sensitized photooxidation of TRP are summarized in Table 1.

Sensitization of TRP^{+} by $Ru(bpy)_3^{2+}/SnO_2$

Adsorption of $Ru(bpy)_3^{2+}$ onto antimony-doped SnO_2 particles results in a quenching of the excited state due to electron injection into the conduction band of the semiconductor. The rate constant of this process (10^9 S^{-1}) is large compared to the intrinsic lifetime of $*Ru(bpy)_3^{2+}$ in aerated H_2O (k_{INTR} = 2.8×10^6 S^{-1}). It has been shown that at the particle- to $Ru(bpy)_3^{2+}$ -complex concentration ratio used, essentially all $Ru(bpy)_3^{2+}$ complexes are adsorbed onto the surface (31) and thus it can be assumed that no $O_2(^1\Delta_g)$ will be produced in this case.

The lifetime of $Ru(bpy)_3^{3+}$ was measured using laser flash photolysis. Photoinjection of an electron into SnO_2 following excitation with λ = 532 nm light, results in a transient bleaching of the ground-state absorbance at λ = 450 nm. The decay back to the initial baseline exhibits a stretched exponential character (Fig. 1), the origin of which is discussed elsewhere (29). It has been described earlier that lifetimes obtained from fits of stretched exponential decay

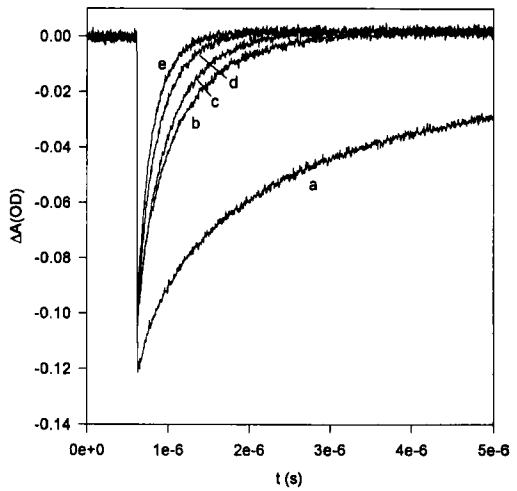

Figure 1. Transient ground-state bleaching and recovery at 450 nm due to the formation and decay of $Ru(bpy)_3^{3+}$ following photoinjection from $Ru(bpy)_3^{2+}$ (23 μM) adsorbed onto antimony-doped SnO_2 particles (12.5 μM) in the absence (a) and in the presence of 2.99 mM (b), 4.21 mM (c), 6.09 mM (d) and 8.87 mM (e) TRP.

curves can be used analogously to single exponential lifetimes to obtain bimolecular rate constants (34,35). Thus the decay was fitted according to the Kohlrausch equation: $f(t) = A_0 \exp[-(t/\tau)^\beta]$ with $0 < \beta \leq 1$. Addition of TRP results in a concentration-dependent decrease of the lifetime of $Ru(bpy)_3^{3+}$ from its intrinsic value τ_0 = (2.5 ± 0.1) μs, which is due solely to the recombination reaction (Eq. 7). The τ and β parameters obtained are listed in Table 2.

$$Ru(bpy)_3^{3+} + e^-(SnO_2) \rightarrow Ru(bpy)_3^{2+},\ k_{REC} \quad (7)$$

$$Ru(bpy)_3^{3+} + TRP \rightarrow Ru(bpy)_3^{2+} + TRP^{+},\ k_Q \quad (8)$$

A bimolecular rate constant of $k_Q = 5.9 \times 10^8$ M^{-1} S^{-1} was obtained from the plot of the rate constant for reduction of $Ru(bpy)_3^{3+}$ by TRP as a function of the TRP concentration (Fig. 2). This value of k_Q is of the same magnitude as the bimolecular rate constant for the oxidation of nitroxyl radicals by $Ru(bpy)_3^{3+}$ (4.9×10^8 M^{-1} S^{-1}) (36), but it is three orders of magnitude higher than that for electron transfer from TRP to the oxidized state of rose bengal adsorbed onto ZnO electrodes reported by Matsumara *et al.* who studied the electron transfer from reductants to oxidized dyes using the potential modulation technique (37).

It has been shown that in many cases the rate constants for the charge-transfer quenching of an excited state of a photosensitizer by chemicals capable of donating an electron depends on the ionization potential of the donor (38–40). The rate constants are dependent on the sensitizer used as well as on the solvent and on the pH (23,24). Several studies have also been performed using eosin, methylene blue or thionine as photosensitizers. Bimolecular rate constants for the electron-transfer quenching of these photosensitizers lie between 3.4×10^8 M^{-1} S^{-1} and 3×10^9 M^{-1} S^{-1} (41). Thus the order of magnitude of the rate constant for the quenching of $Ru(bpy)_3^{3+}$ by TRP is comparable with rate constants measured for the charge-transfer quenching processes between sensitizer triplet states and TRP, *e.g.* rate constants for the initiation of type I pathways.

The quenching of $*Ru(bpy)_3^{2+}$ by antimony-doped SnO_2

Table 2. Stretched exponential lifetime τ and stretching parameter β for the decay of $Ru(bpy)_3^{3+}$ adsorbed onto Sb-doped SnO_2 particles (12.5 μM) in the presence of various TRP concentrations

[TRP] (mM)	τ (μs)	β
0	2.448 ± 0.02	0.59 ± 0.007
2.99	0.454 ± 0.003	0.614 ± 0.005
4.21	0.358 ± 0.004	0.891 ± 0.006
6.09	0.243 ± 0.004	0.946 ± 0.001
8.87	0.176 ± 0.003	0.925 ± 0.017

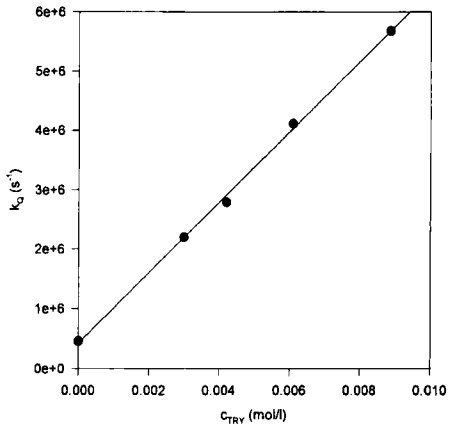

Figure 2. Plot of the reciprocal lifetimes obtained from the fit according to the Kohlrausch equation: $f(t) = A_0[\exp(t/\tau)^\beta]$ (see Table 2) as a function of the TRP concentration.

produces $Ru(bpy)_3^{3+}$ with a quantum efficiency of 0.93 ± 0.01 (36). Thus the quantum yield of $TRP^{\cdot+}$ at the beginning of the photooxidation reaction can be calculated according to

$$\phi_{(TRP^{\cdot+})} = 0.93\frac{k_Q[TRP]}{k_{REC} + k_Q[TRP]}. \quad (9)$$

With the rate constants obtained from the measurements described above $k_Q = 5.9 \times 10^8\ M^{-1}\ S^{-1}$ and $k_{REC} = 4.0 \times 10^5\ S^{-1}$ we obtain an initial quantum yield for the formation of the TRP radical cation of 0.075 when the concentration of TRP is 59.3 μm*M*. The rate constants for the electron-transfer-mediated photooxidation of TRP are summarized in Table 1. Because the TRP concentration decreases as the illumination time increases this is an upper estimation for the $TRP^{\cdot+}$ quantum yield, the order of magnitude of which is comparable to ϕ_Δ.

Products of the $O_2(^1\Delta_g)$ and $TRP^{\cdot+}$-initiated photooxidation reaction of TRP

The distribution of photooxidation products is strongly dependent on the sensitizer, the substrate concentration as well as on the reaction pathway. It has been shown that the product distribution of the photooxidation reaction is strongly influenced by the pH value of the reaction medium. Inoue *et al.* reported that rose bengal-sensitized photooxidation of TRP in aqueous environments at pH 6–7 results mainly in the formation of *N*-formylkynurenine (N-FK) as well as hydroperoxy-hydropyrrole-indole carboxylic acid (HPI) (7). In comparison to the dominantly $O_2(^1\Delta_g)$ pathway sensitized with rose bengal, thionine was used for the type I photooxidation of TRP in their studies. According to their studies, only N-FK and HPI could also be detected as the primary photooxidation products, but the yields differed compared to the product yield of the $O_2(^1\Delta_g)$ pathway (7).

For a qualitative comparison of the product distributions obtained from photosensitization of TRP using $Ru(bpy)_3^{2+}$ free in solution and from $Ru(bpy)_3^{2+}$ adsorbed onto SnO_2, ^{1}H-NMR spectra were measured. Qualitative comparison of the spectra obtained from the two solutions did not show any differences in the product distribution (data not shown). This is consistent with the results of Inoue (7). No attempts were made to analyze the product distribution. Although $Ru(bpy)_3^{2+}$ adsorbed onto SnO_2 is *per se* not a type I photosensitizer because the photooxidation reaction is initiated from the oxidized state of the $Ru(bpy)_3^{2+}$ complex and not from the triplet state, they both result in the formation of $TRP^{\cdot+}$, *i.e.* they should have the same net effect.

Rate constants for the $O_2(^1\Delta_g)$ and electron-transfer-mediated photooxidation of TRP

The rate constant for the $Ru(bpy)_3^{2+}$ and $Ru(bpy)_3^{2+}/SnO_2$-sensitized loss of TRP was measured using fluorescence spectroscopy. The electronic properties of N-FK, one of the likely products of the photooxidation reaction (7) have been characterized by Pileni *et al.* (42). The absorption spectrum of N-FK in H_2O has three maxima at about 225 nm, 260 nm and 315 nm. At the excitation wavelength (290 nm) the absorption coefficients of TRP and N-FK in H_2O are comparable. The fluorescence maxima of N-FK in H_2O (λ_{em} = 450 nm and λ_{em} = 550 nm), however, are significantly red-shifted compared to that of TRP(λ_{em} = 368 nm). Because the fluorescence quantum yield of N-FK is very small ($\phi_{N\text{-}FK}$ = 0.001) (42) the fluorescence intensity at 368 nm can be used for evaluation of the TRP concentration. Figure 3a shows TRP fluorescence emission spectra before and after illumination for 60 s, 120 s, 360 s, 480 s and 1200 s, respectively. The decrease in fluorescence intensity reflects a loss of approximately 29% of the TRP concentration due to the $O_2(^1\Delta_g)$-mediated photooxidation of TRP. The TRP fluorescence emission spectra before and after illumination for 30 s, 60 s, 90 s, and 180 s, respectively, using $Ru(bpy)_3^{2+}$ adsorbed onto SnO_2 as a photosensitizer are shown in Fig. 3b. Photooxidation *via* the radical-mediated pathway results in a faster decrease of the TRP concentration, approximately 48% of TRP being depleted after 120 s. The rate of TRP depletion according to Eqs. 5 and 6 is given by

$$-\frac{d[TRP]}{dt} = \phi_\Delta N_P \frac{k_{c(\Delta)}[TRP]}{k_\Delta^0 + k_t[TRP]} \quad (10)$$

for the $O_2(^1\Delta_g)$ pathway with k_Δ^0 being the rate constant for the intrinsic decay of $O_2(^1\Delta_g)$ in H_2O and N_P the rate of photon absorption. According to Eqs. 7–9 the rate of TRP depletion for the radical pathway is given by

$$-\frac{d[TRP]}{dt} = \phi_{TRP^{\cdot+}} N_P \frac{k_c[TRP]}{k_{REC} + k_Q[TRP]}. \quad (11)$$

Because light scattering effects can be neglected (31), it can be assumed that N_P is equal for both samples. The photooxidation of TRP follows a pseudo-first-order kinetics for both pathways because $k_t[TRP] \ll k_\Delta^0$ and $k_Q[TRP] \ll k_{REC}$.

$$\log\left(\frac{[TRP]_t}{[TRP]_{t=0}}\right)2.303 = -\phi_\Delta N_P \frac{k_{c(\Delta)}}{k_\Delta^0} t \quad (12)$$

$$\log\left(\frac{[TRP]_t}{[TRP]_{t=0}}\right)2.303 = -\phi_{TRP^{\cdot+}} N_P \frac{k_c}{k_{REC}} t. \quad (13)$$

After calculating the TRP concentration from the fluorescence intensity at 368 nm using the slope obtained from the calibration curves, the expressions on the left side of Eqs. 12 and 13 were plotted as a function of the illumination time (Fig. 4a,b). From the slopes of these plots (m = −2.68 ×

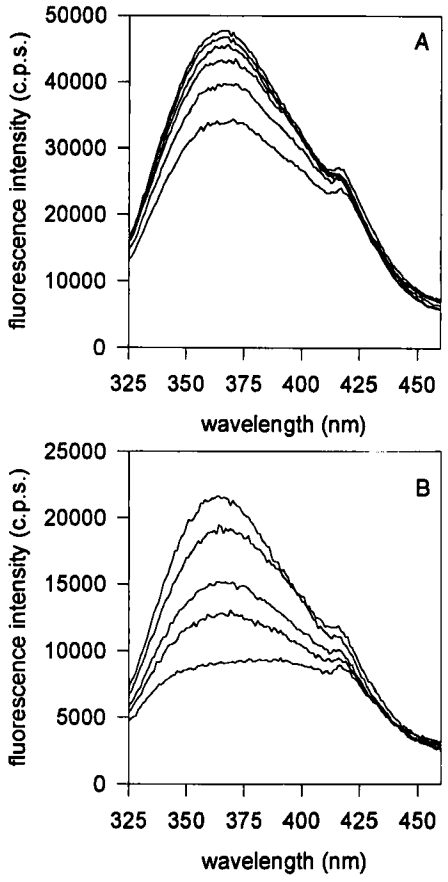

Figure 3. (**a**) Fluorescence emission spectra of TRP (λ_{exc} = 290 nm) after illumination for 0 s, 60 s, 120 s, 360 s, 600 s and 1200 s (top to bottom) with 514 nm (355 mW/cm^2) using $Ru(bpy)_3^{2+}$ in solution as a photosensitizer. (**b**) Fluorescence emission spectra of TRP (λ_{exc} = 290 nm) after illumination for 0 s, 30 s, 60 s, 90 s and 180 s (top to bottom) with 514 nm (355 mW/cm^2) using $Ru(bpy)_3^{2+}$ adsorbed onto SnO_2 particles antimony-doped SnO_2 particles as a photosensitizer.

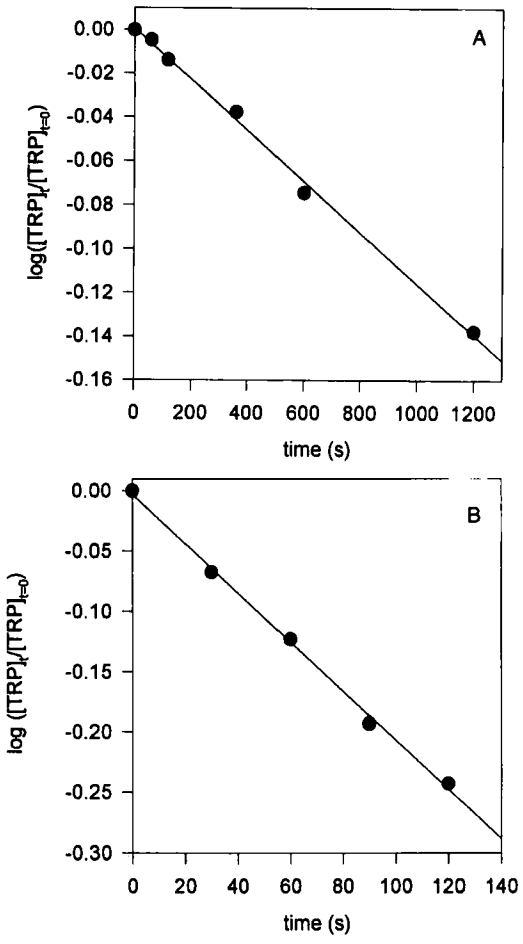

Figure 4. (**a**) Plot of ($\log[TRP]_t/\log[TRP]_{t=0}$) as a function of illumination time for the $O_2(^1\Delta_g)$ pathway. (**b**) Plot of ($\log[TRP]_t/\log[TRP]_{t=0}$) as a function of illumination time for the radical pathway. The TRP concentration was calculated from the fluorescence emission experiments using a different calibration curve for each system.

10^{-4} M^{-1} S^{-1} for the $O_2(^1\Delta_g)$ pathway and m = -4.69×10^{-3} M^{-1} S^{-1} for the radical pathway) the relative rate constants for the photooxidation of TRP were evaluated using $k_\Delta^0 = 2.5 \times 10^5$ S^{-1} and $k_{REC} = 4.0 \times 10^5$ S^{-1}, respectively. This resulted in $k_{c(\Delta)} = (372/N_P)$ M^{-1} S^{-1} for the $O_2(^1\Delta_g)$ pathway and $k_c = (25\,013/N_P)$ M^{-1} S^{-1} for the photooxidation *via* formation of $TRP^{\cdot+}$ radical, respectively. As mentioned above, the quantum yield for the formation of the $TRP^{\cdot+}$ calculated according to Eq. 11 is an upper estimation because [TRP] is not constant. After illumination for 180 s, the TRP concentration decreased by approximately 48%. Accordingly, the quantum yield for $TRP^{\cdot+}$ would be reduced to approximately 0.05 that would lead to $k_c = (37\,600/N_P)$ M^{-1} S^{-1}. The error in k_C introduced through this uncertainty is rather large. An absolute rate constant could not be obtained from these series of experiments because the rate of photon absorption was not measured. Nevertheless, the relative rate constants obtained differ by two orders of magnitude and demonstrate that in the chosen model system, photooxidation of TRP *via* a radical pathway is much more efficient than *via* a singlet oxygen pathway. This result is in line with results of earlier investigations (24,43,44). Two particular aspects of our study distinguish it from the earlier ones: (1) photooxidation occurs exclusively *via* one pathway or the other, and (2) the involvement of the superoxide radical, $O_2^{\cdot-}$, is unlikely.

By comparing lumiflavin (type I) and rose bengal (type II) as sensitizers for the photooxidation of indole (24), Yoshimura and Ohno were able to largely distinguish between the two pathways because the lumiflavin triplet state was predominantly quenched by electron transfer from indole and the rose bengal triplet state was predominantly quenched by energy transfer to O_2. However, $O_2(^1\Delta_g)$ was efficiently formed in the quenching of the lumiflavin triplet by O_2, so that it was impossible to exclude that pathway. In our model system, the photoexcited $Ru(bpy)_3^{2+}$ is not quenched by TRP but rather by either SnO_2 (type I) or O_2 (type II), so that oxidation of TRP occurs exclusively by one pathway or the other.

Lumiflavin-mediated photooxidation also necessarily generates $O_2^{\cdot-}$, which is produced by the reaction of the lumiflavine semiquinone anion radical with O_2 (24). Yoshimura and Ohno regarded $O_2^{\cdot-}$ to react with the indole radical cation to form the oxygenated products. Biological systems are poised for the rapid removal of $O_2^{\cdot-}$, however, so that the

latter may not generally be directly involved in the oxidation process. The conduction band electron that is produced with $Ru(bpy)_3^{3+}$ (Eq. 3) reacts so slowly with O_2 that it does not affect the recapture reaction (Eq. 7), which occurs on the microsecond time scale (29,45). Thus it is more likely that the photooxidation of TRP *via* reaction with $Ru(bpy)_3^{3+}$ (Eq. 8) involves reaction between the TRP radical cation with O_2 than with $O_2^{-\cdot}$. The reaction of TRP radical cation with O_2 is known to produce the same oxidation products as the reaction of TRP with $O_2(^1\Delta_g)$ (7,46,47), as confirmed by our results. Yoshimura and Ohno found that the type I process is more efficient than the competing type II process, which was attributed to the fact that the redox potential of the triplet lumiflavin is higher than the redox potential of Ind^{+}/Ind. In line with these results are also the results on the yields of the riboflavin-sensitized photooxidation of TRP obtained by Silva *et al.* (44).

These studies were performed in a well-chosen model system. It is unlikely that dyes adsorbed onto semiconductor particles can be used for *in vivo* studies. Moreover, as discussed above, the efficiencies for electron transfer reactions between a triplet state of a sensitizer and TRP can vary over several orders of magnitude, and the electron transfer reaction between $Ru(bpy)_3^{3+}$ and TRP is very efficient, with a bimolecular rate constant of $k_Q = 5.9 \times 10^8\ M^{-1}\ S^{-1}$. In addition we would like to point out that there are several photosensitizers with much higher $O_2(^1\Delta_g)$ quantum yields compared to the $Ru(bpy)_3^{2+}$ complex used.

The purpose of this study was a comparison of the photooxidation efficiencies of the $O_2(^1\Delta_g)$-induced pathway with an electron-transfer-induced pathway. The photosensitized radical pathway is not *per se* a type I pathway. The type I pathway as defined implies an electron-transfer quenching reaction between a sensitizer triplet state and a substrate molecule. In this case, the formation of the oxidized state is the result of a fast injection of an e^- into the semiconductor particle (28). The chosen system, however, has the advantage that the rate of photons absorbed is the same in both samples, which allows a direct comparison of the relative rate constants obtained for the depletion of TRP without determination of N_P. The efficiency for photooxidation of biomolecules depends not only on the above-discussed parameters like the rate constants for energy or electron transfer, and the quantum yields for the formation of the oxidizing species. In cellular systems it is also strongly dependent on the localization properties of the photosensitizer and the intracellular concentration. Both can easily be influenced by the side-chain functionalities of a photosensitizer, whereas the photooxidation pathway can be influenced *via* substitution of heavy metals.

Acknowledgements—Support for this work was obtained from the NIH (grant GM24235). J. M. Wessels thanks the Alexander von Humboldt foundation for support within the Feodor-Lynen Program.

REFERENCES

1. Foote, C. S. (1976) Photosensitized oxidation and singlet oxygen: consequences in biological systems. In *Free Radicals in Biology*, Vol. II (Edited by W. A. Pryor), pp. 85–113. Academic Press, New York.
2. Balasubramanian, D., X. Du and J. S. Zigler, Jr. (1990) The reaction of singlet oxygen with proteins, with special reference to crystallins. *Photochem. Photobiol.* **52**, 761–768.
3. Cozzani, I. and G. Jori (1980) Photooxidation of L-glutamate decarboxylase from *Escherichia coli*, sensitized by the coenzyme pyridoxal phosphate and by proflavine. *Biochim. Biophys. Acta* **623**, 84–88.
4. Jori, G. (1975) Photosensitized reactions of amino acids. *Photochem. Photobiol.* **21**, 463–467.
5. Tsai, C. S., J. R. P. Godin and A. J. Wand (1985) Dye sensitized photo-oxidation of enzymes. *Biochem. J.* **225**, 203–208.
6. Matheson, I. B. C. and J. Lee (1979) Chemical reaction rates of amino acids with singlet oxygen. *Photochem. Photobiol.* **29**, 879–881.
7. Inoue, K., T. Matsuura and I. Saito (1982) Mechanism of dye-sensitized photooxidation of tryptophan, tryptamine and their derivatives. Singlet oxygen process in competition with type I process. *Bull. Chem. Soc. Jpn.* **55**, 2959–2964.
8. Silva, E., V. Rückert, E. Lissi and E. Albuin (1991) Effects of pH and ionic micelles on the riboflavin-sensitized photoprocesses of tryptophan in aqueous solution. *J. Photochem. Photobiol. B Biol.* **11**, 57–68.
9. Lindig, B. A. and M. A. J. Rodgers (1981) Rate parameters for the quenching of singlet oxygen by water-soluble and lipid-soluble substrates in aqueous and micellar systems. *Photochem. Photobiol.* **33**, 627–634.
10. Reddi, E., M. A. J. Rodgers, J. D. Spikes and G. Jori (1984) The effect of medium polarity on the hematoporphyrin-sensitized photooxidation of L-tryptophan. *Photochem. Photobiol.* **40**, 415–421.
11. Smith, G. J. (1978) Photooxidation of tryptophan sensitized by methylene blue. *J. Chem. Soc. Faraday Trans.* **74**, 1350–1354.
12. Spikes, J. D. and M. L. MacKnight (1979) Dye sensitized photooxidation of proteins. *Ann. N.Y. Acad. Sci.* **171**, 149–162.
13. Goosey, J. D., J. S. Ziegler and J. H. Hinoshita (1980) Cross-linking of lens crystallins in a photodynamic system: a process mediated by singlet oxygen. *Science* **208**, 1270.
14. Lissi, E. A., M. V. Encinas, E. Lemp and M. A. Rubio (1993) Singlet oxygen $O_2(^1\Delta_g)$ bimolecular processes. Solvent and compartmentalization effects. *Chem. Rev.* **93**, 699–723.
15. Mandal, K., M. Kono, S. K. Bose, J. Thomson and B. Chakrabarti (1988) Structure and stability of γ-crystallins—VI. Aggregation and structural destabilization in photosensitized reactions. *Photochem. Photobiol.* **47**, 583–591.
16. Saito, I., T. Matsuura, M. Nakagawa and T. Hino (1977) Peroxidation intermediates in photosensitized oxygenation of tryptophan derivatives. *Acc. Chem. Res.* **10**, 346–352.
17. Nilsson, R., P. B. Merkel and D. R. Kearns (1972) Unambiguous evidence for the participation of singlet oxygen ($^1\Delta$) in photodynamic oxidation of amino acids. *Photochem. Photobiol.* **16**, 117–124.
18. Calhoun, D. B., J. M. Vanderkooi and S. W. Englander (1983) Penetration of small molecules into proteins studied by quenching of phosphorescence and fluorescence. *Biochemistry* **22**, 1533–1539.
19. Bertolotti, S. G., N. A. García and G. A. Argüello (1991) Effect of the peptide bond on the singlet-molecular-oxygen-mediated photo-oxidation of tryptophan dipeptides. A kinetic study. *J. Photochem. Photobiol. B Biol.* **10**, 57–70.
20. Michaeli, A. and J. Feitelson (1994) Reactivity of singlet oxygen toward amino acids and peptides. *Photochem. Photobiol.* **59**, 284–289.
21. Michaeli, A. and J. Feitelson (1994) Reactivity of singlet oxygen toward large peptides. *Photochem. Photobiol.* **61**, 255–260.
22. Palumbo, M. C., N. A. Garcia and G. A. Argüello (1990) The interaction of singlet molecular oxygen $O_2(^1\Delta_g)$ with indolic derivatives. Distinction between physical and reactive quenching. *J. Photochem. Photobiol. B Biol.* **7**, 33–42.
23. Ferraudi, G., G. A. Argüello, H. Ali and J. E. van Lier (1988) Type I and II photooxidation of amino acids by phthalocyanines: a flash photochemical study. *Photochem. Photobiol.* **47**, 657–660.
24. Yoshimura, A. and T. Ohno (1988) Lumiflavin-sensitized photooxygenation of indole. *Photochem. Photobiol.* **48**, 561–565.

25. Rodgers, M. A. J. (1993) Reflections on type I photodynamic damage. *J. Photochem. Photobiol. B* **18**, 296–298.
26. Mulazzani, Q. G., H. Sun, M. Z. Hoffman, W. E. Ford and M. A. J. Rodgers (1994) Quenching of the excited states of ruthenium(II)–diimine complexes by oxygen. *J. Phys. Chem.* **98**, 1145–1150.
27. Zhang, X. and M. A. J. Rodgers (1995) Energy and electron transfer reactions of the MLCT state of ruthenium tris(bipyridyl) with molecular oxygen: a laser flash photolysis study. *J. Phys. Chem.* **99**, 12797–12803.
28. Lin, D., G. L. Hug and P. V. Kamat (1995) Photochemistry on surfaces. Intermolecular energy and electron transfer processes between excited $Ru(bpy)_3^{2+}$ and H-aggregates of cresyl violet on SiO_2 and SnO_2 colloids. *J. Phys. Chem.* **99**, 16768–16775.
29. Ford, W. E., J. M. Wessels and M. A. J. (1997) Rodgers Electron injection by photoexcited Ru $(bpy)_3^{2+}$ into colloidal SnO_2: analysis of the recombination kinetics based on electrochemical and Auger capture models. *J. Phys. Chem.* (In press)
30. Harriman, A. (1987) Further comments on the redox potentials of tryptophan and tyrosine. *J. Phys. Chem.* **91**, 6102–6104.
31. Ford, W. E., J. M. Wessels and M. A. J. Rodgers (1996) Time-resolved luminescence investigation of the adsorption of $Ru(bpy)_3^{2+}$ onto antimony-doped SnO_2 colloidal particles. *Langmuir* **12**, 3449–3453.
32. Tanielian, C., H. Muller and L. Golder (1984) Dye-sensitized photooxidation of tryptophan. In *Oxygen Radicals in Chemistry and Biology* (Edited by W. Bors, M. Saran and D. Tait), pp. 551–554. Walter de Gruyter, Berlin.
33. Matheson, I. B. C., R. D. Etheridge, N. R. Kratowich and J. Lee (1975) The quenching of singlet oxygen by amino acids and proteins. *Photochem. Photobiol.* **21**, 165–171.
34. Ford, W. E. and M. A. J. Rodgers (1994) Interfacial electron transfer in colloidal SnO_2 hydrosyls photosensitized by electrostatically and covalently attached ruthenium (II) polypyridine complexes. *J. Phys. Chem.* **98**, 3822–3831.
35. Kelly, L. A. and M. A. J. Rodgers (1994) Reductive quenching of novel mixed-ligand tris(bipyridyl)ruthenium(II) complexes in aqueous solution and inert colloidal suspensions. *J. Phys. Chem.* **98**, 6377–6385.
36. Ford, W. E. and M. A. J. Rodgers (1997) Kinetics of nitroxyl radical oxidation by $Ru(bpy)_3^{3+}$ following photosensitization of antimony-doped tin dioxide colloidal particles. *J. Phys. Chem.* (In press)
37. Matsumara, M., K. Mitsuda and H. Tsubomura (1983) Dye sensitization of a zinc oxide electrode studied by a potential modulation technique. *J. Phys. Chem.* **87**, 5248–5251.
38. Cohen, S. G., A. Parola and G. H. Parsons, (1973) Photoreduction by amines. *Chem. Rev.* **73**, 141–161.
39. Kayser, R. H. and R. H. Young (1976) Photoreduction of methylene blue by amines—I. A flash photolysis study of the reaction between triplet methylene blue and amines. *Photochem. Photobiol.* **24**, 395–401.
40. Rehm, D. and A. Weller (1969) Kinetics and mechanism of electron transfer in fluorescence quenching in acetonitrile. *Ber. Bunsenges. Phys. Chem.* **73**, 834–839.
41. Usui, Y. and H. Koizumi (1967) An interpretation of the photochemical behavior of dye-reducing agent-oxygen system on the basis of a switch-over of the primary processes. *Bull. Chem. Soc. Jpn.* **40**, 440–446.
42. Pileni, M.-P., P. Walrant and R. Santus (1976) Electronic properties of *N*-formylkynurenine and related compounds. *J. Phys. Chem.* **80**, 1804–1809.
43. Amat-Guerri, F. and R. Martínez-Utrilla (1990) Direct and dye-sensitized aqueous photooxidation of 3-indoleacetic acid, methyl-3-indoleacetate and 1-methyl-3-indoleacetic acid. II: quantum yields and mechanism. *J. Photochem. Photobiol. A Chem.* **50**, 377–387.
44. Silva, E., S. Rissi and K. Dose (1974) Photo-oxidation of lysozyme at different wavelengths. *Radiat. Environ. Biophys.* **11**, 111–124.
45. Ford, W. E. and M. A. J. Rodgers (1994) Interfacial electron transfer in colloidal SnO_2 hydrosols photosensitized by electrostatically and covalently attached ruthenium(II) polypyridine complexes. *J. Phys. Chem.* **98**, 3822–3831.
46. Singh, A., S. A. Antonson, G. W. Koroll, W. Kremers and H. Singh (1984) Radicals and photolysis of aqueous aerated tryptophan solutions. In *Oxygen Radicals in Chemistry and Biology* (Edited by W. Bors, M. Saran and D. Tait), pp. 491–498. Walter de Gruyter, Berlin.
47. Maskos, Z., J. D. Rush and W. H. Koppenol (1992) The hydroxylation of tryptophan. *Arch. Biochem. Biophys.* **296**, 514–520.